PERGAMON

Building and Environment 36 (2001) 351–358

BUILDING AND ENVIRONMENT

www.elsevier.com/locate/buildenv

CFD analysis and energy simulation of a gymnasium

Joseph C. Lam[a,*], Apple L.S. Chan[b]

[a]*Building Energy Research Group, Department of Building and Construction, City University of Hong Kong, Tat Chee Avenue, Kowloon, Hong Kong*

[b]*Division of Building Science and Technology, City University of Hong Kong, Tat Chee Avenue, Kowloon, Hong Kong*

Received 12 July 1999; received in revised form 27 September 1999; accepted 10 January 2000

Abstract

A computational fluid dynamics (CFD) program EXACT3 has been applied to investigate the temperature distribution and air movement within an air-conditioned gymnasium with four different, but commonly found, exhaust positions in Hong Kong. In this numerical study, the effects of thermal stratification on the energy performance (in terms of cooling load and electricity consumption) are examined with respect to the HVAC plant oversizing issue. It has been found that significant thermal stratification occurs in the gymnasium. The annual cooling load can be overestimated by 45.4% for the best exhaust position when the effect of thermal stratification is not considered. The corresponding peak cooling load and, hence, chiller plant size, will increase from 59.9 to 77.6 kW. The low energy efficiency of the oversized chiller at part-load operation results in a 7% increase in the annual energy use for the HVAC plant.

Keywords: Computational fluid dynamics analysis; BLAST energy simulation; Air stratification; HVAC oversizing; Gymnasium

1. Introduction

Hong Kong, as one of the leading financial and banking centres, has seen rapid economic growth in the past two decades. Average household incomes rose from HK$1700 (1 US$=HK$7.8, approximately) in 1971 to HK$16,400 in 1993, an increase of 865% over the 23-year period [1]. As the society becomes more affluent and living standards improve, there has been a growing demand for top quality recreational facilities. The indoor gymnasium has become one of the favourite venues for local indoor sport activities. The growing desire for better thermal comfort in the indoor gymnasium through air-conditioning has resulted in a marked increase in energy consumption in this sector. Under an air-conditioned situation, significant thermal stratification exists in an indoor gymnasium with high ceiling height. The occupied zone is cooled by conditioned air while warm air accumulates near the ceiling. Most of the heating, ventilating and air-conditioning (HVAC) thermal load simulation programs currently used in design practices, are based on a one-air-point temperature connected with the walls, floor and ceiling by means of convective heat transfer resistances. The calculated cooling load tends to be overestimated and, hence, the HVAC plant oversized, resulting in low energy efficiency at part-load operation [2,3].

Fig. 1 shows the electricity used in the non-domestic building sector from 1971–1993. It can be seen that electricity consumption rose from 1780 GWh in 1971 to 14,759 GWh in 1993, representing an average annual rate of increase of 10.1% [1]. Because of the growing concern about the energy consumption and its likely implications for the environment in Hong Kong, there is a need for a more detailed and systematic study on the energy performance of buildings, particularly fully air-conditioned non-domestic buildings with a large enclosed space. In the past two decades, a com-

* Corresponding author. Tel.: +852-2788-7609; fax: +852-2788-7612.

E-mail address: bcexem@cityu.edu.hk (J.C. Lam).

0360-1323/00/$ - see front matter
PII: S0360-1323(00)00014-7

Nomenclature

a_m thermal diffusivity of a CPAC monier tile (m^2 s^{-1})
a_g thermal diffusivity of gypsum board (m^2 s^{-1})
A surface area of an RSC (m^2)
C_D discharge coefficient
C_g specific heat of gypsum board (J kg^{-1} $°C^{-1}$)
C_m specific heat of a CPAC monier tile (J kg^{-1} $°C^{-1}$)
C_p specific heat at constant pressure of air (J kg^{-1} $°C^{-1}$)
d_g thickness of gypsum board (m)
d_m thickness of a CPAC monier tile (m)
g gravitational acceleration, 9.81 m s^{-2}
G_{ap} gap size between CPAC monier tiles and gypsum board (m)
Gr Grashof number
H air gap between CPAC monier tiles and gypsum board (m)
h the time in hours
h_1 convection heat transfer coefficient from the upper surface of the roof induced by wind (W m^{-2} $°C^{-1}$)
h_3 free convection heat transfer coefficient from lower surface of a monier plate to moving air (W m^{-2} $°C^{-1}$)
h_4 free convection heat transfer coefficient from upper surface of a gypsum plate to moving air (W m^{-2} $°C^{-1}$)
h_6 convection heat transfer coefficient from the lower surface of a gypsum plate to the interior (W m^{-2} $°C^{-1}$)
I_t hourly monthly mean global radiation intensity incident on the RSC (W m^{-2})
k_f thermal conductivity of moving air (W m^{-1} $°C^{-1}$)
k_g thermal conductivity of gypsum board (W m^{-1} $°C^{-1}$)
k_m thermal conductivity of a CPAC monier tile (W m^{-1} $°C^{-1}$)
L length of the RSC (m)
$\dot{m}$ mass flow rate of moving air (kg s^{-1})
Nu Nusselt number
Pr Prandtl number
t time (s)
T_a ambient temperature (K)
T_f mean temperature of moving air $\{T_f = [(T_o + T_i)/2]\}$ (K)
T_i inlet incoming air temperature of the RSC ($T_i = T_r$) (K)
T_o outlet temperature of air, outcoming from the RSC (K)
T_r room temperature (K)
T_s equivalent sky temperature (K)
T_1 upper surface temperature of a CPAC monier tile (K)
T_2 center temperature of a CPAC monier tile (K)
T_3 lower surface temperature of a CPAC monier tile (K)
T_4 upper surface temperature of gypsum board (K)
T_5 center temperature of gypsum board (K)
T_6 lower surface temperature of gypsum board (K)
V wind velocity (m s^{-1})
W width of the RSC (m)
X_m axis along the thickness of a CPAC monier tile
X_g axis along the thickness of gypsum board

Greek symbols

α absorptivity of a CPAC monier tile
ϵ_g thermal emissivity of gypsum board
ϵ_m thermal emissivity of a CPAC monier tile
θ tilt angle of the RSC (°)
ρ density of air (kg m^{-3})
ρ_g density of gypsum board (kg m^{-3})
ρ_m density of a CPAC monier tile (kg m^{-3})
σ Stefan–Boltzmann constant, 5.669×10^{-8} (W m^{-2} K^{-4})

concluded that this configuration would make the optimum natural ventilation and allow a long duration of operating. Gypsum board is used not only due to its low thermal conductivity, but mainly due to its low price and wide people acceptance.

The width of the RSC was set equal to 100 cm. The characteristic and thermal properties of materials are given in Table 1.

For modeling the RSC, the following simplifying assumptions were made:

1. there is a one-dimensional heat flow through the absorber plate (monier tiles), as well as throu backing insulation (gypsum board);
2. the length L is considered to be large when cc pared with the air gap, H;
3. the heat capacity of solid materials are consider i.e., heat transfer is under unsteady state conditio
4. the effect of corrugation of CPAC monier tile: neglected, i.e., the cross-section of the air channe assumed to be rectangular and shading is negligil
5. properties of air are functions of temperature;
6. the heat transfer fluid is regarded as non-radia

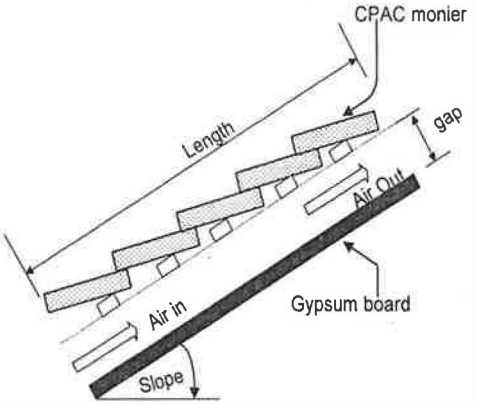

Fig. 1. Schematic representation of the RSC.

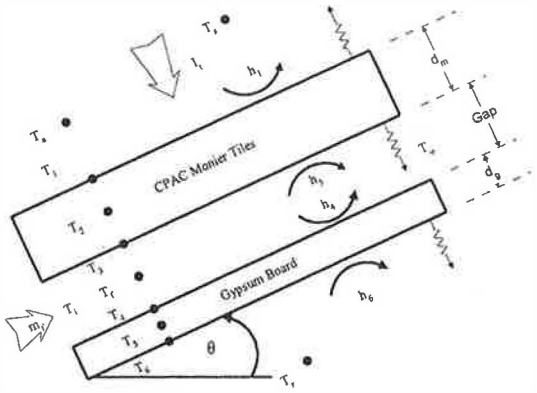

Fig. 2. Node and heat transfer exchanges through the RSC.

absorption;
7. the sky can be considered as a black body for long wavelength radiation at an equivalent sky temperature;
8. loss through the front and rear are for the same ambient temperature;
9. the air leakage effect is negligible;
10. properties of materials are temperature independent;
11. dust and dirt on the RSC are negligible.

Based on the combination of three modes of heat transfer, a nodal formulation of the RSC system is provided by performing an energy balance at each node of the RSC (Fig. 2). The transient energy equation on each node of each component is listed below.

Monier tile

• At $x_m = 0$

$$\alpha I_t + h_1(T_a - T_1) + \epsilon_m \sigma(T_s^4 - T_1^4) + k_m \frac{\partial T_m}{\partial x_m} = \rho_m C_m \frac{\Delta x_m}{2} \frac{\partial T_1}{\partial t} \quad (1)$$

I_t is the hourly monthly mean global radiation includ both the direct and diffuse radiations. Computation is made based on the approach most commonly used.

• At $0 < x_m < d_m$

$$\frac{\partial T_m(x, t)}{\partial t} = a_m \frac{\partial^2 T_m}{\partial x^2} \quad (2)$$

• At $x_m = d_m$

$$h_3(T_f - T_3) + \sigma \frac{(T_4^4 - T_3^4)}{\frac{1}{\epsilon_m} + \frac{1}{\epsilon_g} - 1} + k_m \frac{\partial T_m}{\partial x_m} = \rho_m C_m \frac{\Delta x_m}{2} \frac{\partial T_3}{\partial t} \quad (3)$$

Gypsum board

• At $x_g = 0$

$$h_4(T_f - T_4) + \sigma \frac{(T_3^4 - T_4^4)}{\frac{1}{\epsilon_m} + \frac{1}{\epsilon_g} - 1} + k_g \frac{\partial T_g}{\partial x_g} = \rho_g C_g \frac{\Delta x_g}{2} \frac{\partial T_4}{\partial t} \quad (4)$$

• At $0 < x_g < d_g$

$$\frac{\partial T_g(x, t)}{\partial t} = a_g \frac{\partial^2 T_g}{\partial x^2} \quad (5)$$

• At $x_g = d_g$

$$h_6(T_f - T_6) + \epsilon_g \sigma(T_r^4 - T_6^4) + k_g \frac{\partial T_g}{\partial x_g} = \rho_g C_g \frac{\Delta x_g}{2} \frac{\partial T_6}{\partial t} \quad (6)$$

Table 1
The characteristic and thermal properties of materials

Material	Dimension (cm) (thickness)	Thermal conductivity ($W\ m^{-1}\ K^{-1}$)	Thermal emissivity	Thermal absorptivity	Thermal diffusivity ($m^3\ s^{-1}$)
Monier tile	1.5	0.1463	0.93	0.77	0.93
Gypsum board	0.9	0.0873	0.903	–	–

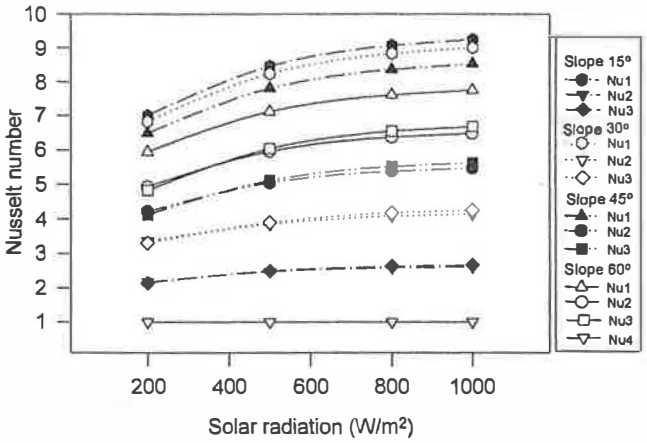

Fig. 3. Variations of the Nusselt number calculated with different correlations vs solar radiation for different tilt angles of the RSC (gap: 0.14 m; length: 2 m).

Moving air

$$h_3(T_3 - T_f) + h_4(T_4 - T_f) + \frac{\dot{m}}{A} C_p(T_i - T_o) = 0 \qquad (7)$$

The mass flow rate of air induced by the RSC chimney can be estimated by using the following equation [7]

$$\dot{m} = C_D \rho H W \sqrt{gL \sin(\theta) \frac{(T_o - T_i)}{T_i}} \qquad (8)$$

The heat transfer coefficient for wind-related heat loss, from the top plate of roof, was calculated from a correlation presented by McAdam [5]

$$h_1 = 2.8 + 3.0V \qquad (9)$$

where V is the wind velocity (m s^{-1}).

At the lower surface of the gypsum board, for a down facing hot plate, the following equation was used [8]

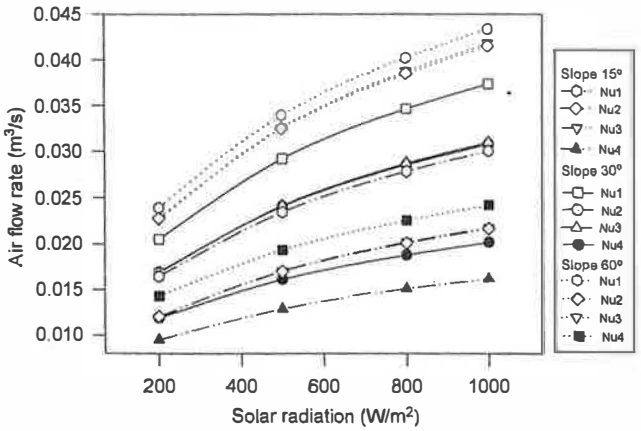

Fig. 4. Variations of the air flow rate vs solar radiation for three tilt angles of the RSC (15, 30 and 60°; gap: 0.14 m; length: 2 m).

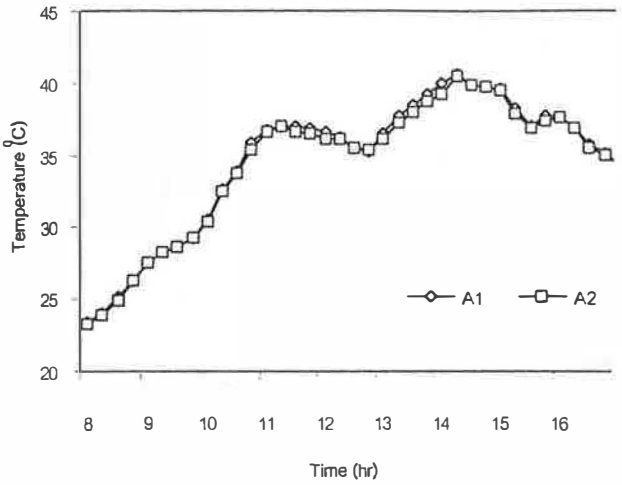

Fig. 5. Air gap temperatures at two positions at equal distance fro the inlet of the RSC (gap = 0.14 m, 13/12/96).

$$h_6 = 1.42[\sin\ \theta(T_6 - T_r)/L]^{0.25} \qquad (1$$

The natural convection heat transfer coefficients c both sides of the RSC air channel are assumed to l equal:

$$h_3 = h_4 = Nu\ k_f/H \qquad (1$$

Although free convection, theoretically and/or empi cally, has been treated extensively and has suppli different correlations, the free convection heat transfe with tilted parallel plate channels that are open to t ambient at opposite ends and where the hot plate the upper one, has not been studied extensively. Ther fore, to evaluate the Nusselt correlation (Nu), v focus analysis on the free convection heat transf inside an enclosed rectangular cavity, in which the tv opposing walls are maintained at different temper

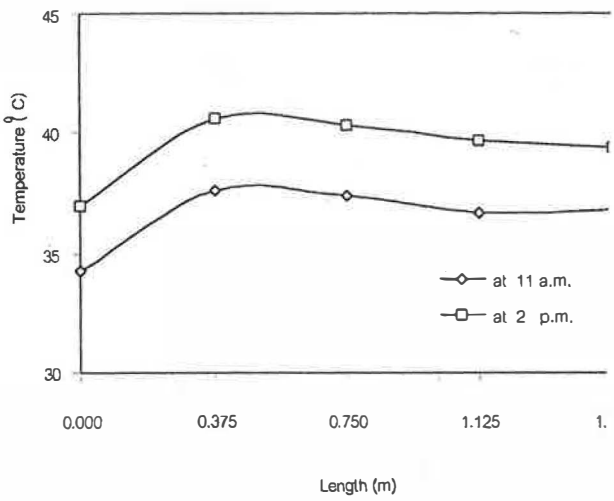

Fig. 6. Longitudinal temperature of the RSC air temperature at t different times (gap = 0.14 m, 13/12/96).

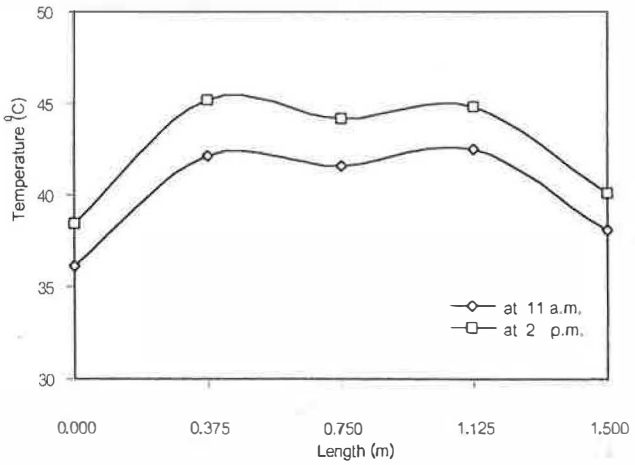

Fig. 7. Longitudinal temperature of a CPAC monier tile at two different times (gap = 0.14 m, 13/12/96).

tures. In fact, that is a reasonable approximation because of the lower expected values of the air flow rate.

The above system of equations has been solved by using the explicit method of finite-difference with a straightforward scheme [9]. The grid distance along the CPAC monier tiles and gypsum board was equal to half of the material thickness, i.e., $\Delta x_m = (d_m/2)$; $\Delta x_g = (d_g/2)$. The time step was 20 s and the stability requirement was calculated as follows: $[\alpha(\Delta t/\Delta x^2)]$.

3. Numerical results

The air properties are evaluated based on linear regression [10]. The ambient conditions (solar radiation, ambient temperature, wind velocity) used are those based on data of Bangkok.

Three characteristic months (March, July and November) representing the three different seasons in Thailand (winter, hot–hot and monsoon) were considered, respectively. Each month was represented by its characteristic day, determined according to the average day with the extraterrestrial radiation closest to the average for the month [5].

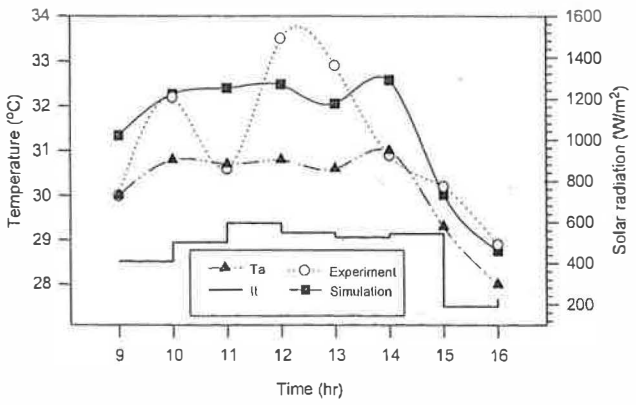

Fig. 8. Hourly variation of the RSC air temperature and ambient conditions (length: 2 m; gap: 0.14 m; 19/8/94).

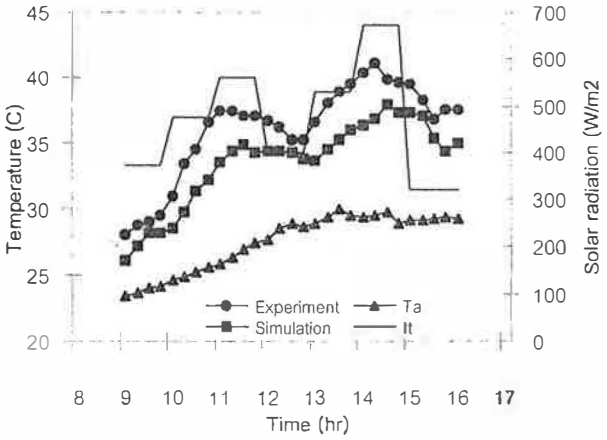

Fig. 9. Hourly variation of the RSC air temperature and ambient conditions (length: 1.5 m; gap: 0.14 m; 13/12/96).

3.1. Preliminary result

Testing the effect of the Nusselt number correlations has been done in order to find the appropriate one for our RSC model. Four correlations were selected, the first correlation ($Nu1$), applied for a flat plate solar collector proposed by Holland et al. [5]. The second correlation ($Nu2$) is the natural convection correlation in an inclined rectangular enclosure for an aspect ratio in the range $2 \leq (H/L) \leq 10$ and for tilt angles from $90° < \theta < 180°$ [11]. The third correlation ($Nu3$), which has been suggested in [12], is for all aspect ratios and for the Grashof number $2.1 \times 10^5 < Gr < 1.1 \times 10^7$. On the other hand, depending on operating conditions, we expected the Rayleigh number to be small. That implies the buoyancy-driven flow is weak and the heat transfer is predominantly by conduction effect. Hence, the Nusselt number is unity ($Nu4$).

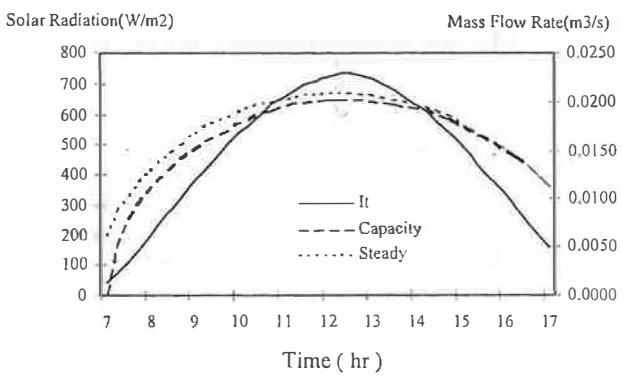

Fig. 10. Comparison between steady and transient models of the RSC.

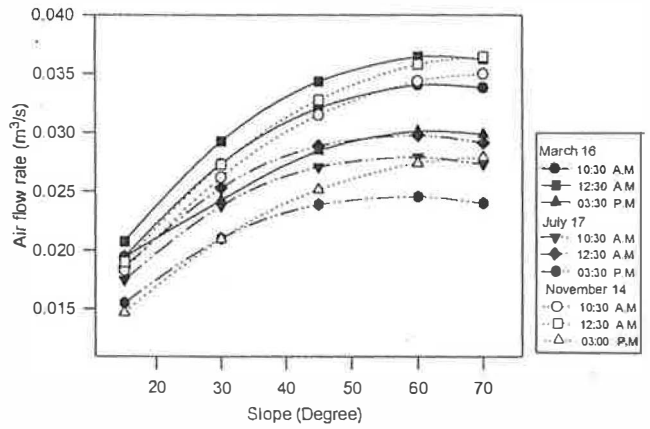

Fig. 11. Variations of the air flow rate vs the slope of the RSC for different months at different times (gap: 0.14 m; length: 2 m).

As indicated in Figs. 3 and 4, the value of $Nu4$ and the air flow rate calculated with the correlation $Nu4$ is close to those of the other values except for a low slope and low solar radiation. Therefore, $Nu4$ cannot be used for our model because the intensity of solar radiation in Thailand is very high and the roof tilt angle of the habitation is often higher than 15°.

Even though the value of $Nu1$ is higher than those of the other correlations, it is not appropriate for our case because the formula was developed for applications involving a cool surface on the upper side of the cavity, as for the flat plate solar collector.

Finally, the values of the Nusselt number, calculated by using $Nu2$ and $Nu3$ correlations, are similar. Therefore, $Nu2$ or $Nu3$ correlations could be used to estimate the natural air flow rate.

In order to analyze the performance of the RSC system, correlation $Nu3$ is selected because it can be used for all aspect ratios (H/L). Therefore, the following expression for the Nusselt number is

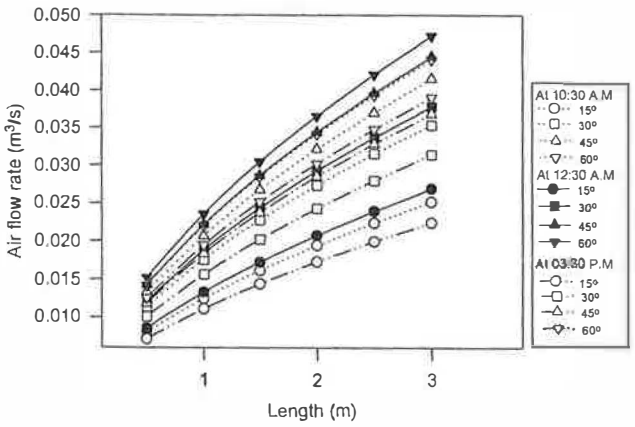

Fig. 12. Variations of the air flow rate with the length of the RSC at three different times for different slopes (17 March; gap: 0.14 m).

Table 2
Specific air flow rate induced by one module of the model[a]

Month	Specific air flow rate (m^3/s)			
	Model A	Model B	Model C	Model D
March	0.0416	0.0619	0.0666	0.0713
July	0.0361	0.0537	0.0566	0.0597
November	0.0389	0.0578	0.0633	0.0685

[a] One module is a unit width and has one flat plate (Model A) or different flat plate sections (Models B, C and D).

$$Nu3 = 1 + \left\{0.071(Gr\ Pr)^{1/3}\left[\frac{H}{L}\right]^{-1/9} - 1\right\} \sin\ \theta \qquad (12)$$

The effect of air gap H was also investigated. It was found that the higher H is, the higher the induced ventilation rate. However, beyond 14 cm, the assumptions made would not be valid and heat losses through lateral sides of the RSC have to be included. Thus, an air gap of about 10 to 14 cm seems to be a reasonable choice.

3.2. Validation of numerical model

Before comparing experimental and numerical results, an initial validation of the assumption of a one-dimensional heat transfer model is discussed below, based only on experimental results.

From Fig. 5, it can be seen that the temperature of the air gap at two different positions at equal distance from the inlet, namely $A1$ and $A2$, are uniform. Also Figs. 6 and 7 indicate that, except at the ends of the RSC, the temperature of the air and gap side of the CPAC monier tile were quite constant. Therefore assuming a uniform temperature, along the width of

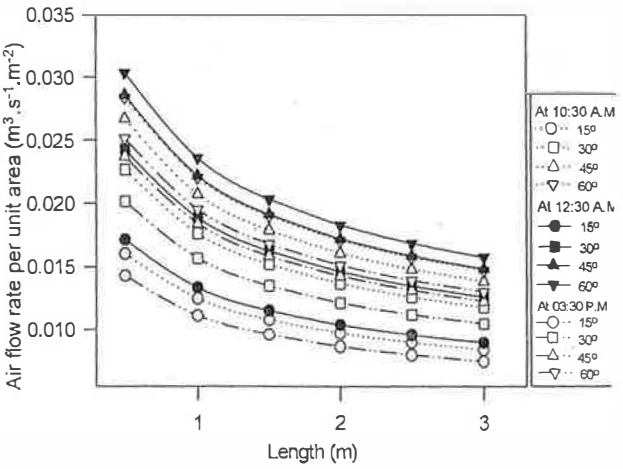

Fig. 13. Variation of the air flow rate per unit area of the RSC the length at different times for different slopes (17 March; ga 0.14 m).

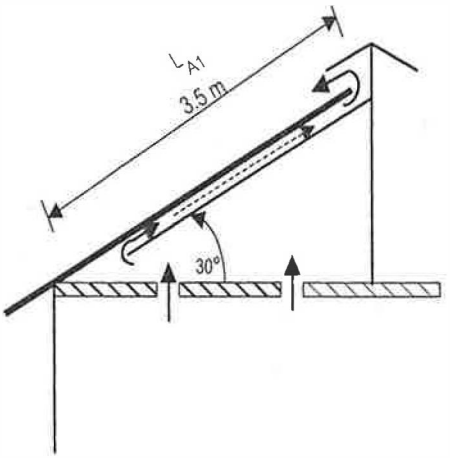

Fig. 14. Schematic view of Model A.

the RSC, a one-dimension of heat transfer is acceptable.

Figs. 8 and 9 show that for two different days and the calculated results of air, the RSC temperature followed the ambient conditions. It can be seen that there are few disagreements with the measured data [4,6]. This is mainly due to the effect of variability of ambient conditions during each hour — the ambient conditions were recorded on an hourly basis and wind which was not accounted for in the model — and the fact that the experimental profiles plotted here are the average of measured temperatures at different positions. However, regarding the weak temperature difference between the simulated and experimental RSC air profile, and also with the quite weak wind speed (about 1.5 m/s for Bangkok), the developed numerical model can be considered as a good approximation for estimating the long-term performance of the RSC.

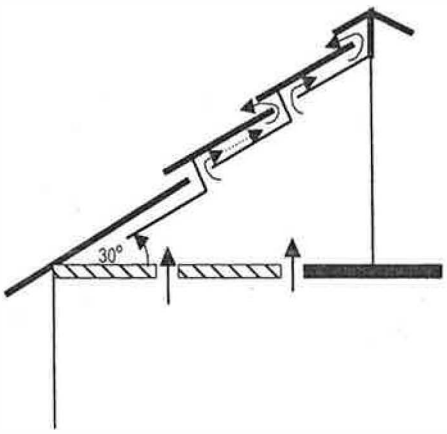

Fig. 15. Schematic view of Model B.

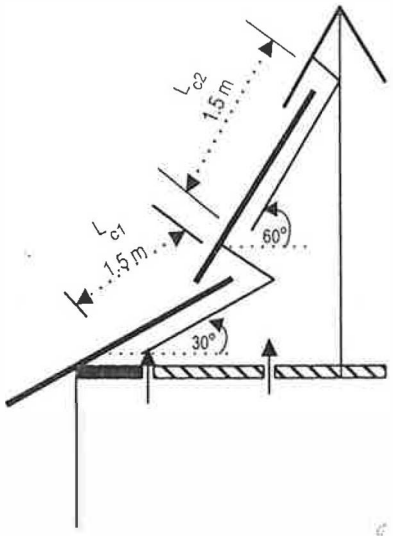

Fig. 16. Schematic view of Model C.

3.3. Effect of the RSC parameters

The results are presented parametrically by selecting a base case and varying one parameter at a time, whereas the other RSC parameters are kept constant. In this study, the air inlet and outlet surface areas were considered equal, and the width and gap of the RSC were fixed at 100 and 14 cm, respectively.

3.3.1. Thermal capacity of the CPAC monier tile

Regarding the small thickness of materials, it is expected that the thermal capacity of solid materials could be neglected. Fig. 10 shows that calculating mass flow rate under steady state conditions yields to higher value, especially at the beginning of the simulation as the heat capacity effect is neglected. Heat sto-

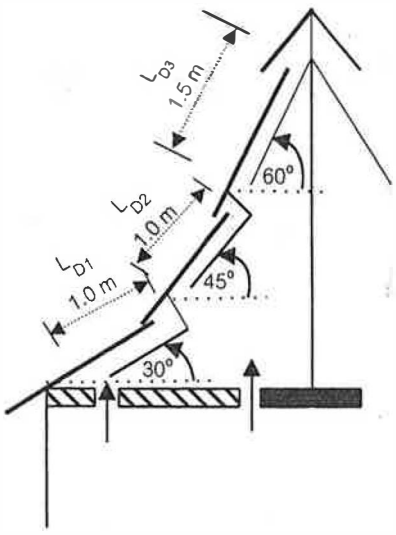

Fig. 17. Schematic view of Model D.

rage within the CPAC monier tile delays the heat transfer into the air gap. In the afternoon, where enough heat is stored and solar intensity decreased, the induced mass flow rate is nearly similar. Thus, with regard to sizing of the RSC, the thermal capacity of the CPAC monier tile could also be neglected.

3.3.2. Slope of the RSC

Fig. 11 shows that the induced air flow rate is a function of the slope and the intensity of solar radiation. Up to 30°, the induced air flow rate increased rapidly by increasing the tilt angle. However, the vertical height is still too small to induce higher air flow rate, although the energy absorbed by the tiles is higher. For $\theta > 60°$, the increase of the air flow rate was quite insignificant. Consequently, for further designs of RSC systems, the appropriate range of tilt angle should be considered between 20 and 60°.

3.3.3. Length of the RSC

Fig. 12 shows that for all slopes, increasing the length of the RSC increased the air flow rate, which is a consequence of the increased vertical height of the ventilation path.

However, as shown in Fig. 13, the air flow rate per unit area decreased with increasing length of the RSC. Thus, the amount of air flow rate induced by one longer RSC would be lower than that induced by two units of the RSC, with a total length equal to that of the longer unit. Therefore, to maximize the air ventilation by the RSC systems, the length of the RSC should be shorter, in the order of 100–200 cm. This length could be selected by architects, depending on the available surface area of roof. This result agreed well with that presented in [6].

4. Design of new configurations of passive roof solar collector

Based on preceding results, the RSC concept can be used to induce a natural air circulation within the roof structure, which consequently will reduce the heat accumulation under the roof.

In this study, we propose four different design configurations of a passive roof solar collector. Figs. 14 and 15 are exactly the same as those now used by an architect. They are adapted to act as an RSC, which has only one plate (Fig. 14) or different short flat plate sections (Fig. 15).

The traditional Thai house, with a high gable roof, extended long eaves and harmonious integration with the environment, was well designed to promote natural ventilation, which provided a natural feeling of comfort [13]. Thus, the last two configurations are proposed, to design in the traditional Thai style, as shown in Figs. 16 and 17. But the appearance of Model D is closer to the traditional Thai roof [14].

By knowing the daily average ambient conditions and specific cross-section of the house, the required rate of ventilation demand or the number of air change (ACH) could be estimated. Then, by using the developed numerical model of the RSC, the specific induced amounts of total air flow rate by the different models can be estimated. They are given in Table 2. It can be seen that for all seasonal months, the total air flow rate of Model D, which is close to the traditional Thai roof, was higher than that of the other models.

It can also be seen that the total ventilation rate is quite small. Thus, it may not be enough to provide certain feelings of comfort. However, if the effect of wind has been taken into account, the air flow rate should be bigger, twice at least, as investigated by Awbi [3]. Therefore, it may be reasonable to expect a certain feeling of comfort for the residents, especially if RSC systems were also coupled to a modified Trombe wall's system.

Consequently, for further design, a configuration could be selected by designers and architects depending on a good compromise between cost and energy saving.

5. Conclusion

A Roof Solar Collector can provide a significant part of ventilation and air flow rate in houses. The proposed configuration of the RSC system has to be verified with full scale testing. With only the RSC system, there is little potential to induce sufficient natural ventilation to satisfy the resident's comfort. However, if it is coupled with other passive cooling devices, such as the Trombe wall, the cooling efficiency will be improved considerably.

Comparison of the RSC performance with a classical flat plate collector used as a ventilator — though not shown here — would give more satisfaction. namely with regard to system cost and simplicity.

Acknowledgements

The authors thank the National Research Counci of Thailand (NRCT) for the partial support of thi work.

References

[1] Barozzi GS, Imbabi MSE, Nobile E, Sausa ACM. Physical an numerical modeling of a solar chimney-based ventilation syster for building. Building and Environment 1992;27(4):433–45.

[2] Bansal NK. Solar chimney for enhanced stack ventilation. Building and Environment 1993;28(3):373–7.
[3] Awbi HB. Design considerations for naturally ventilated buildings. Renewable Energy 1994;5:1081–90.
[4] Bunnag T. A study of a Roof Solar Collector towards the natural ventilation of new habitations. Thesis, Master of Engineering, Thermal Technology Program, King Mongkut's Institute of Technology Thonburi, 1995.
[5] Duffie JA, Beckmann WA. Solar engineering of thermal processes. New York: Wiley, 1980.
[6] Khedari J, Hirunlabh J, Bunnag T. Experimental study of a roof solar collector towards the natural ventilation of new habitations. In: World Renewable Energy Congress, Denver, 1996. p. 335–8.
[7] Donald W, Abrams PE. Low energy cooling. New York: Van Nostrand Reinhold, 1986.
[8] Suwantragul B, Watabutr W, Sitathani K, Tia V, Namprakai P. Solar and wind energy potential assessment of Thailand. Renewable Nonconventional Energy Project, USAED Project No. 493-0304, Solar and Wind Resource Assessment Component, King Mongkut's Institute of Technology Thonburi, pp. 423–433, 1984.
[9] Wylie C Ray, Barrett C Louis. Advanced engineering numerical methods. New York: McGraw-Hill, 1982.
[10] Wachirapuwadon S. An adapted model of a passive solar collector for new houses with respect to traditional Thai style. Thesis, Master of Science, Energy Technology Program, King Mongkut's Institute of Technology Thonburi, 1996.
[11] Incropera FP, DeWitt DP. Fundamentals of heat and mass transfer. New York: Wiley, 1996.
[12] Gebhart B. Heat transfer. 2nd ed. New York: McGraw-Hill, 1971.
[13] Buranasomphob T. Energy conservation in building design: a case study of a traditional style house. In: ASEAN-EC Energy Conservation Seminar, Bangkok, 1987. p. 177–81.
[14] Yuktasewewiwad L. The shape of a traditional Thai roof. Agson-Jarearntad, 1977. p. 1–40.